JPET Fast Forward. Published on December 5, 2005 as DOI: 10.1124/jpet.105.092916

Improving the *In vitro* Prediction of *In vivo* CNS Penetration: Integrating Permeability, Pgp Efflux and Free Fractions in Blood and Brain.

Scott G Summerfield, Alexander J Stevens, Leanne Cutler, Maria del Carmen Osuna, Beverley Hammond, Sac-Pham Tang, Ann Hersey, David J Spalding, Phil Jeffrey.

Drug Metabolism and Pharmacokinetics Department, Neurology and Gastrointestinal Centre of Excellence for Drug Discovery, GlaxoSmithKline R&D, New Frontiers Science Park, Third Avenue, Harlow, Essex, CM19 5AW. (SGS, AJS, LC, MCO, BH, SPT, DJS, PJ).

Computational Chemistry, GSK Medicines Research Centre, Gunnels Wood Road, Stevenage, Hertfordshire, SG1 2NY. (AH)

Improving the *In vitro* Prediction of *In vivo* CNS Penetration.

Corresponding author: Scott Summerfield, Drug Metabolism and Pharmacokinetics Department, Neurology and Gastrointestinal Centre of Excellence for Drug Discovery, GlaxoSmithKline R&D, New Frontiers Science Park, Third Avenue, Harlow, Essex, CM19 5AW.

Tel: +44 (0)1279 627926

Fax +44 (0)1279 622727

Email: Scott.G.Summerfield@GSK.com

Abbreviations: BBB, blood-brain barrier; Br:Bl, brain:blood concentration ratio; Papp, apparent membrane permeability; Kbb, *in vitro* brain:blood partition ratio.

No. Text pages: 20

No. Tables: 4

No. figures: 6

No. words (Abstract): 200

No. words (Introduction): 739

No. words (Discussion): 953

Abstract

This work examines the inter relationship between the unbound drug fractions in blood and brain homogenate, passive membrane permeability, Pgp efflux ratio and cLogP in determining the extent of CNS penetration observed *in vivo*. The present results demonstrate that compounds often considered to be Pgp substrates in rodents (efflux ratio greater than 5 in MDR-MDCK cells) with poor passive permeability may still exhibit reasonable CNS penetration *in vivo*, i.e. where the unbound fractions and non-specific tissue binding act as a compensating force. In these instances, the efflux ratio and *in vitro* blood-brain partition ratio (Kbb) may be used to predict the *in vivo* blood-brain ratio. This relationship may be extended to account for the differences in CNS penetration observed *in vivo* between mdr1a/b wild type and knockout mice. In some instances cross-species differences that might initially appear to be related to differing transporter expression can be rationalised from knowledge of unbound fractions alone. The results presented in this manuscript suggest that the information exists to provide a coherent picture of the nature of CNS penetration in the Drug Discovery setting, allowing the focus to be shifted away from understanding CNS penetration toward the more important aspect of understanding CNS efficacy.

Introduction

Within the modern Drug Discovery paradigm, Drug Metabolism and Pharmacokinetics (DMPK) play an integral role in the process of compound selection and progression. Much of the impact of DMPK has been due to its transformation from a largely descriptive discipline to that of a predictive science, fuelled by advances in bioanalysis and *in vitro* techniques. Hence Discovery DMPK provides a powerful means for assessing the risks of taking potential assets into Development.

Nevertheless, the development of molecules targeted at the central nervous system (CNS) remains a significant challenge due to the increased regulation and protection afforded to the brain over other organs of the body. The major knowledge gaps are (1) understanding the physicochemical features that determine CNS penetration (2) understanding the impact of the blood-brain barrier (BBB) on CNS uptake and (3) providing a coherent measure of CNS penetration that can be related to drug efficacy. Regarding the latter point, whilst it is important to develop a link between the pharmacokinetics of a molecule and the biophase, arguably the critical issue is one of sufficient access of free drug to the requisite site of action.

Numerous models and measures of CNS uptake are available to assist in the search for centrally-active agents. In situ brain perfusion techniques have highlighted the good correlation between increasing lipophilicity and CNS permeability. Polar drugs that are subject to paracellular absorption such as atenolol (log $D_{oct,7.4}$ -2.1; Artursson, 1990) and sumatriptan (log$D_{oct,7.4}$ -1.5; Pascual and Munoz (2005) show minimal brain permeability due to the tight junction morphology at the BBB. Lipophilic compounds (i.e. propranolol, log $D_{oct,7.4}$ 1.2, Artursson, 1990), able to undergo passive transcellular diffusion in the unbound, unoinised form show improved BBB permeability relative to atenolol (Street et al.

1979). Outliers to this trend are often substrates for either influx of efflux transporters (Smith, 2003; Kuresh et al., 2004). Of particular note is P-glycoprotein (Pgp), whose promiscuous role in modulating the brain penetration of many therapeutic agents has been the subject of extensive research (Lin, 2004; Lin, 2003; Mahar Doan et al., 2002).

Assessing the extent of Pgp efflux on CNS uptake may be obtained from either *in vitro* BBB models, such as Madin Darby Canine Kidney (MDCK) cells overexpressing the human form of Pgp, or *in vivo* models by comparing the CNS penetration in mdr1/a(+/+) mice to mdr1a/b(-/-) knockouts. From these *in vitro* methods the efflux ratio (ER) is generally determined, defined as the fold difference between the basolateral to apical (B-A) transfer rate of drug across a cell monolayer relative to its apical to basolateral (A-B) rate of transfer. In general molecules exhibiting good passive membrane permeability and low efflux ratios (i.e. < 2) tend to exhibit good CNS penetration *in vivo*. The cut-off for permeability is dependent upon the nature of the assay format, i.e. cell density, but usually these values are between 30 nm/s (Wang et al., 2005) and 200 nm/s (Mahar Doan et al., 2002).

Other measures of CNS penetration include brain/plasma (Br:Pl) or similarly brain/blood (Br:Bl) ratios from bulk tissue, cerebrospinal fluid (CSF) concentrations (Shen et al., 2004)) or interstitial fluid (ISF) concentrations measured *via* microdialysis (De Lange et al., 1997; Langer et al, 2004), with the former two techniques offering better throughput to the meet the demands in Drug Discovery. Recently, however, equilibrium dialysis has been reported as an alternative means of assessing unbound drug in brain tissue. Studies in rodents (Kalvass and Maurer, 2002; Maurer et al., 2005) have provided a reasonably good prediction of the brain-plasma ratios for compounds where the blood-brain barrier does not modulate CNS penetration (Doran et al., 2005). Despite the fact that the use of tissue homogenates results

in the mixing of intracellular and extracellular elements, improved correlations have been reported between Br:Pl ratios and CSF concentrations with the incorporation of fu(brain).

In this study we have extended the utility of equilibrium dialysis to include the effect of transporters. We report correlations of the unbound fraction in blood and brain and the *in vitro* Br:Bl partition ratio (Kbb) with several key parameters; efflux ratio, clopP and *in vivo* Br:Bl ratios derived from the mdr1a/b knockout mouse model. Combining measurements of Kbb and efflux ratio markedly improves the *in vitro* prediction of *in vivo* CNS penetration for Pgp substrates in rats. The trend can be extended to account for differences in CNS penetration between wild type and KO mice, highlighting the quantitative physiological relevance of the efflux ratio.

Materials and Methods

The following compounds were obtained from the Sigma Chemical Company (Poole, Dorset, UK); paracetamol, ketorolac, ibuprofen, atenolol, flurbiprofen, indomethacin, naproxen, diclofenac. All other compounds were available from in house sources.

Calculated Physicochemical Properties

Log octanol/water partition coefficients (clogP) were calculated using CLOGP software, Biobyte Corporation, Claremont, California. Calculations of pKa values (denoted as ApKa1and BpKa1 for acid and base dissociation) was performed with PKALC Version 3.11 CompuDrug Chemistry Ltd, Budapest, Hungary. Calculation of Polar surface area (PSA) was based on the work of Clark (1999).

Equilibrium Dialysis Measurements

The methodology employed in this study was a modification of that reported by (Kalvass et al., 2002). Briefly, a 96-well equilibrium dialysis apparatus was used to determine the free-fraction in the blood and brain for each drug (HT Dialysis LLC, Gales Ferry, CT, USA). Membranes (3kDA cut-off) membranes were conditioned in deionized water for 40 min, followed by conditioning in 80:20 deionised water:ethanol for 20 min, and then rinsed in deionised water before use. Rat blood and brain were obtained fresh on the day of the experiment. Blood was diluted 1:1 with PBS while the brain tissue was homogenised with PBS to a final composition of 1:2 brain:PBS, by means of ultrasonication (Tomtec Autogiser, Receptor Technologies, Adderbury, Oxon, UK) in an ice bath. Diluted blood and brain homogenate were spiked with the test compound (1000 ng/g) and 100-µl aliquots (n = 6 replicate determinations) were loaded into the 96-well equilibrium dialysis plate. Dialysis versus PBS (100 uL) was carried out for 5h in a temperature controlled incubator at 37°C

(Stuart Scientific, Watford, UK), using an orbital microplate shaker at 125 rev/min (Stuart Scientific, Watford, UK). At the end of the incubation period, aliquots of blood, brain homogenate or PBS were transferred to Matrix ScreenMate tubes (Matrix Technologies, Hudson, NH, USA), and the composition in each tube was balanced with control fluid such that the volume of PBS to blood or brain was the same. Sample extraction was performed by the addition of 200 uL of acetonitrile containing an internal standard. Samples were allowed to mix for 15 minutes and then centrifuged at 2465 x g in 96-well blocks for 20 min (Eppendorf 5810R, VWR International, Poole, Dorset, UK). The unbound fraction was determined as the ratio of the peak area in buffer to that in blood or brain, with correction for dilution factor according to equation 1 (Kalvass and Maurer, 2002).

$$fu = \frac{(1/D)}{(1 - fu(apparent) + 1/D} \quad (1)$$

where, D = dilution factor in blood or brain homogenate and fu(apparent) is the measured free fraction of diluted blood or brain tissue.

As described by Kalvass and Maurer (2002), if the unbound fractions in blood and brain are equal at steady state then the in vivo Br:Bl ratio can be estimated from free-fractions in blood and brain tissue as follows,

$$\frac{fu(blood)}{fu(brain)} = \frac{C(brain)}{C(blood)} \quad (2)$$

Where fu(blood) and fu(brain) denote the unbound fractions in blood and brain. The *in vitro* brain:blood partition ratio, fu(blood)/fu(brain) is termed Kbb in this manuscript.

Analysis of Test Compounds in Equilibrium Dialysis.

All samples were analysed by means of HPLC/MS/MS on a PE-Sciex API-4000 tandem quadrupole mass spectrometer (Applied Biosystems, Ontario, Canada), employing a Turbo V

Ionspray operated at a source temperature of 700°C, (80 psi of nitrogen). Samples (3-10 µl) were injected using a CTC Analytics HTS Pal autosampler (Presearch, Hitchin, UK) onto a Hypersil Aquastar 3.0 x 30 mm, 3-µm column (Thermo, Runcorn, Cheshire, UK) operated at 40°C and at an eluent flow rate of 1 mL/min. Analytes were eluted using a high-pressure linear gradient program, by means of an HP1100 binary HPLC system (Agilent, Stockport, Cheshire, UK), using acetonitrile as solvent B. For HPLC/MS/MS analysis in positive ion mode solvent A comprised 1mM ammonium acetate containing 0.1% (v/v) formic acid, while in negative ion mode solvent A comprised 1 mM ammonium acetate. The gradient was held at 5% solvent B for 2 min, before increasing to 90% at 1.2 min, remaining at 90% until 1.6 min before returning to the starting conditions. The cycle time was 2.5 min per sample. Relative peak areas between the PBS and tissue half-wells were used to determine the respective free fractions.

Apparent Permeability and Pgp Efflux Measurements.

All permeability and Pgp efflux measurements were performed as described previously (Wang et al., 2005). Briefly, MDR-MDCK monolayers were grown to confluence on collagen-coated, microporous, polycarbonate membranes in 12-well Costar Transwell® plates. The buffer used was Hanks Balanced Salt Solution (HBSS) containing 10 mM HEPES and 15 mM glucose at pH 7.4, and permeability was assessed in the presence and absence of 2 µM Pgp inhibitor GF120918A. All cells were pre-incubated for 30 min and, for the studies using the Pgp inhibitor, GF120918A (Lentz et al., 2000) was present on both sides of the membrane during the incubation and permeation period. Dosing solution concentrations were 3 µM in assay buffer. Cells were dosed on the apical side (A-B) or basolateral side (B-A), and incubated at 37˚C in 5% (v/v) CO_2 in a humidified incubator. Each determination was performed in triplicate. There was a single 60 min sampling time

point. Permeability through a cell-free (blank) membrane was determined to assess non-specific binding to the device and free diffusion of the test compounds through the filter. Membrane transfer of Lucifer yellow was also measured for each monolayer after being subjected to the test articles to assess the integrity of the cell monolayers. All samples were assayed by HPLC/MS/MS using electrospray ionization. Accompanying each set of test compounds, atenolol, pindolol, propranolol and digoxin were also run as positive controls.

The apparent permeability, P_{app}, and percent recovery were calculated according to equations 3 and 4:

$$Papp = \frac{dCr}{dt} \bullet \frac{Vr}{(A \cdot Co)} \tag{3}$$

$$Percent\ \text{Recovery} = 100 \bullet \left(\frac{(Vr \cdot Crfinal) + (Vd \cdot Cdfinal)}{Vd \cdot Co} \right) \tag{4}$$

where,

dC_r/dt is the slope of the cumulative concentration in the receiver compartment versus time in $\mu M\ s^{-1}$.

V_r is the volume of the receiver compartment in cm^3.

V_d is the volume of the donor compartment in cm^3.

A is the area of the cell monolayer (1.13 cm^2 for 12-well Transwell®).

C_0 is the concentration of the dosing solution in μM.

C_r^{final} is the cumulative receiver concentration in μM at the end of the incubation period.

C_d^{final} is the concentration of the donor in μM at the end of the incubation period.

Determination of Steady State CNS penetration in mdr1a/b(+/+) and mdr1a/b(-/-) Mice.

Each mouse (at least 6 weeks old at the time of surgery) was cannulated via the jugular vein (for drug administration) whilst under isoflurane anaesthesia, with the cannulae exteriorised

at the back of the neck. Animals were placed in a jacket and tether counter-balance system and allowed to recover for at least 3 days prior to dosing. Three male control mdr1a/b (+/+) and 3 male mdr1a/b (-/-) knockout mice were dosed with each compound.

The dose solution for each test compound was prepared on the day of dosing using an appropriate formulation for intravenous administration. The infusion rate and infusion time required to reach steady state blood concentrations (taken as at least 3.5 half-lives) were determined separately for each compound, and were based on prior studies to establish the intravenous pharmacokinetics. Blood samples (25 uL) were taken from the tail vein at 0.5 h intervals during the last 2 h of the infusion to confirm steady-state blood concentrations had been achieved. At the end of the infusion period the mice were decapitated and the brain removed and homogenised with an equal weight of purified water (ELGA maxima, ELGA LabWater, High Wycombe, United Kingdom). Triplicate weighed aliquots (50 µL) of brain homogenate were stored at ca. -80°C prior to HPLC/MS/MS analysis. Samples were extracted by a method based on protein precipitation using acetonitrile (250uL containing a suitable internal standard). Brain concentrations were corrected for residual blood volume using 15uL/g of brain tissue as the vascular space (Brown et al., 1986).

Determination of CNS Penetration in the Rat at Steady-State or Following Acute Dosing

The CNS penetration for most compounds (47 of 56) was assessed under steady-state conditions following intravenous administration. The time required reach to steady blood concentrations (taken as at least 3.5 half-lives) was determined from prior studies of the intravenous pharmacokinetics of individual compounds. In some cases, blood and brain concentrations were obtained from acute single time point studies, where sampling was obtained at Cmax.

For steady-state infusion studies, each rat was cannulated via the jugular vein (for drug administration) and femoral vein (for blood sampling) whilst under isoflurane anaesthesia, the cannulae being exteriorised at the back of the neck. Animals were placed in a jacket and tether and allowed to recover for at least 2 days prior to dosing.

The dose solution for each test compound was prepared on the day of dosing using an appropriate formulation for intravenous administration. The infusion rate and infusion time were determined separately for each compound. Blood samples were taken at 0.5 h intervals during the last 2 h of the infusion to confirm steady-state blood concentrations had been achieved. At the end of the infusion period the rats were exsanguinated, decapitated and the brain removed. Blood samples (ca. 80 µL) were collected into tubes containing K_2EDTA as anti-coagulant and aliquoted immediately after collection. An aliquot (50 µL) of each blood sample was diluted with an equal volume of purified water and stored at ca. -80°C to await analysis. Each brain was homogenised with an equal weight of purified water (ELGA maxima, ELGA LabWater, High Wycombe, United Kingdom). Weighed aliquots (50 µL) of brain homogenate were taken and stored at ca. 80°C prior to HPLC/MS/MS analysis.

Samples were extracted by a method based on protein precipitation using acetonitrile (250uL containing a suitable internal standard). Brain concentrations were corrected for residual blood volume using 15uL/g as the vascular space (Brown et al., 1986).

Bioanalysis of Blood and Brain Homogenate Extracts.

In all cases the sample extraction of blood and brain homogenate was performed by a method based on protein precipitation, using acetonitrile (250 uL) containing a structural analogue of the analyte of interest. Extracts were vortex mixed for 20 minutes followed by centrifugation at 2465 x g for 20 minutes (Eppendorf 5810R, VWR International, Poole, Dorset, UK).

Blood and brain extracts were analysed by means of HPLC/MS/MS either PE-Sciex API-4000 or API-3000 tandem quadrupole mass spectrometers (Applied Biosystems, Ontario, Canada), employing a Turbo V Ionspray. For API-3000 methods the interface temperature was set to 450 °C, with an ionspray voltage of 1500 – 2000V. For API-4000 methods the interface temperature operated at 700°C, with an ionspray voltage of 1500 – 2000V. Samples (3-10 µl) were injected using a CTC Analytics HTS Pal autosampler (Presearch, Hitchin, UK) and chromatographed by means of an HP1100 binary HPLC system (Agilent, Stockport, Cheshire, UK). Specific chromatographic conditions were developed for each analyte to complement their physicochemical properties. The following conditions were common to all assays; column temperature of 40°C, eluent flow rate of 1 mL/min with 250 uL/min of eluent flow directed to MS interface, assay run times 2.5 – 3 minutes per samples. Calibration curves were constructed in blood and brain homogenate to cover at least three orders of magnitude (i.e. 5 – 5000 ng/mL). Three calibration points per decade were included together with quality controls covering the concentration range of calibration.

Results

Table 1 details the compound set examined in the present analysis, which was selected to include both marketed and proprietary compounds covering a wide range of physicochemical properties and therapeutic targets within the Neuroscience portfolio. The extent of CNS penetration varies across this compound set from those with poor brain uptake (Br:Bl ratio <0.05:1) to those showing good distribution into the brain (Br:Bl ratio ca. 4:1), following correction for the vascular volume. Lipophilicity ranges across ten orders of magnitude (cLogP -1.9 to 7.9) with a molecular weight range spanning 150 to 550 Da including neutral, acidic and basic compounds as well as substrates for Pgp (comprising twelve compounds spanning six different therapeutic targets).

Results from Equilibrium Dialysis and Non-Specific Binding Measurements

The influence of free fraction on *in vivo* CNS penetration in the rat is highlighted in Figures 1a and 1b. As shown in Figure 1a, the free drug fraction in blood exhibits a weak correlation with *in vivo* Br:Bl ratio ($R^2 = 0.05$), and notably, the CNS penetration of highly protein bound drugs (i.e. fu(blood) < 0.1%) is not restricted by the fraction of unbound drug in the systemic circulation. In contrast, the correlation is improved by taking account of the free fractions in both blood and brain, i.e. Kbb (Figure 1b, $R^2 = 0.54$ for non Pgp substrates). Analogous to the findings of Kalvass and Maurer (2002), the relative tissue affinities of blood and brain play an important role in determining the extent of CNS observed *in vivo*. As such, compounds with free fractions in blood as low as those of GSK-18 and GSK-33 (0.009% and 0.07% free, respectively) may still exhibit good CNS penetration due to the fact that the drug's affinity for brain tissue is higher still (0.006% and 0.03% free, respectively).

Figure 2 shows a plot of fu(brain) versus fu(blood) highlighting three data series, namely Pgp substrates, acids (calculated pKa < 7.4) and non-acids. Eleven of the twelve Pgp substrates are non-acids and the relationship between fu(brain) and fu(blood) is similar to the other non-acids depicted in Figure 2 (combined least square linear relationship, $y = 1.0685x + 0.0403$, $R^2 = 0.8161$). For the acidic compounds, however, some separation is noted whereby acidic compounds tend to exhibit a lower free fraction in blood relative to brain (least square linear relationship, $y = 0.0666x + 0.0011$, $R^2 = 0.6664$). Similarly, the acidic Pgp substrate GSK-11 (ApKa 4.3) shows comparable behaviour to the other acidic compounds within the set. Consistent with the observation that the volume of distribution for acids is lower than that of non-acids (Benet et al. (1996)), these results are consistent with the fact that acidic compounds exhibit a high affinity for blood proteins, such as albumin.

Of the non-acid compounds, five appear to exhibit fu(blood) values that more closely resemble those of the acid series. Two of these compounds are characterised by ApKa's slightly greater than 7.4 and therefore would still be partially ionised in the acid form at physiological pH (i.e. valdecoxib (ApKa 8.8) and celecoxib (ApKa 9.5). The remaining three outliers are GSK-37, 38 and 39, where their respective fu(blood) values (0.0004 to 0.0011) also lead to unexpectedly low Br:Bl ratios in the rat. These compounds will be discussed further with respect to differences in CNS penetration across species.

Correlation Between Efflux Ratio and *In vitro* Brain:Blood Partition Ratio

For the Pgp substrates present in the compound set, Br:Bl ratios ranged from 0.03:1 to 4:1, indicating that although this transporter limits CNS penetration it does not always preclude it entirely. Table 2 shows that the efflux ratios were found to range from ca. 7 to 125 with apparent membrane permeabilities ranging from 2 to 115 nm/s (i.e. in the absence of a Pgp

inhibitor, GF120918) and passive membrane permeabilities from 15 and 350 nm/s (i.e. in the presence of the inhibitor). For seven of the twelve Pgp substrates shown in Figure 1b, Kbb tends to over predict the Br:Bl ratio observed *in vivo*. This is consistent with the fact that the determination of Kbb assumes that the unbound concentrations in the blood and brain compartments are the same at equilibrium, which would only be valid for compounds where the BBB does not influence drug uptake.

Table 2 also shows that the efflux ratio does not appear to be strong a predictor of *in vivo* CNS penetration. Two compounds (GSK-2 and GSK-3) have Papp's lower than 10 nm/s and efflux ratios of ca. 70, which is generally considered to be an indicator for poor CNS penetration. Both compounds, however, exhibited Br:Bl ratios of ca. 0.5:1. Furthermore, several other compounds identified as having high efflux ratios were also found to have an *in vivo* Br:Bl ratio greater than 1.5:1, albeit with higher passive membrane permeabilities. Hence, although there are certainly many good examples where low passive permeability and high efflux ratio translate into poor CNS penetration, there are examples where these parameters do not adequately describe the extent of CNS penetration observed *in vivo*, indicating a role for other parameters in determining the CNS penetration of the particular compounds.

Figure 3 shows a graphical plot of the relationship between *in vivo* Br:Bl ratio and the combination of two *in vitro* parameters, namely the *in vitro* blood-brain partition coefficient (Kbb) and the efflux ratio (ER). A good linear correlation is observed for the twelve Pgp substrates ($R^2 = 0.93$) with a slope of 10.71 and a small y-intercept (-0.19). Despite the efflux ratio being derived from an MDCK cell line expressing human Pgp, Figure 3 shows that there is acceptable agreement with the *in vivo* rat data presented. The good correlation

(R^2 = 0.93) also indicates that two *in vitro* parameters may be used to adequately describe the extent of *in vivo* CNS penetration of these Pgp substrates, i.e. that the Kbb estimates the extent of partitioning between blood and brain tissue while the efflux ratio acts as a correction for the blood-brain barrier component of Pgp efflux. The non-zero intercept may be a result of the fact that *in vivo* rat Br:Bl data is related to human Pgp efflux, Ohe et al. (2005) observed a similar y-intercept discrepancy which improved on the use a cell line expressing rodent Pgp (mdr1a).

The correlation between Br:Bl ratio and Kbb/ER suggests that an improved *in vitro* estimate of *in vivo* CNS penetration may be derived by means of the linear equation shown in Figure 3, in which both partitioning and efflux ratio are accounted for:

$$ER\ corrected\ in\ vitro\ BB\ partition\ ratio = \left(10.707 \cdot \frac{Kbb}{ER}\right) - 0.1949 \qquad (5)$$

Figure 4 depicts a plot of rat Kbb values against *in vivo* Br:Bl ratio, where the Kbb for the Pgp substrates have been corrected for their efflux ratios. Comparison of Figures 1b and 4 highlight the point that combining the information on both the efflux ratio and Kbb markedly improves the *in vitro* prediction of CNS penetration for Pgp substrates. This is true not only for the substrates where Pgp is seen to exert a large impact on the CNS penetration (i.e. GSK-4, GSK-5) but also for substrates where CNS penetration was not markedly affected by Pgp (i.e. GSK-1, GSK-9). Linear regression shows that the line of best fit for Kbb and Br:Bl ratio yields a slope less than unity (ca. 0.94) and a negative y-intercept of -0.13 (R^2 0.75).

Correlations of Efflux Ratio with CNS Penetration in the mdr1a/b(+/+) and mdr1a/b(-/-) Mouse Model.

The well accepted gold standard method for determining the Pgp status of a drug is the fold difference in Br:Bl ratio between wild type mice and their knockout counterparts, where Pgp is not present. The physiological relevance of the *in vitro* measurement of efflux ratio is further exemplified when comparing the *in vivo* CNS penetration between mdr1a/b(+/+) mice with mdr1a/b(-/-) knockouts, shown in Table 3. The extent of CNS penetration in for mdr1a/b(+/+) mice may be determined from mdr1a/b(-/-) corrected by the *in vitro* efflux ratio. Figure 5 shows a plot of the Br:Bl ratio from mdr1a/b(-/-) mice corrected for efflux ratio against the Br:Bl ratio from mdr1a/b(+/+) mice, where a strong correlation ($R^2 = 0.96$) is observed in analogy to the *in vitro* relationship depicted in Figure 3. Hence although the efflux ratio is derived from a relatively simple model of the blood-brain barrier, the present data suggest that the value can be used quantitatively to account for the CNS penetration observed *in vivo* relative to either Pgp knockouts models or to *in vitro* measurements of brain:blood partitioning.

Species Differences Rationalised by i*n vitro* Brain:Blood Partitioning

As discussed above, although Pgp efflux is a major factor limiting CNS penetration *in vivo*, the physicochemical properties of a molecule may also limit brain uptake. In a recent drug discovery project, a species mismatch appeared for one compound class whereby appropriate efficacy was demonstrated in the guinea pig model while proving ineffective in the rat version of the same PD model. Prior knowledge of the cloned receptors suggested that this was not a consequence of target differences, since previous compounds had elicited pharmacological responses in both species. Analysis of blood and brain samples from these studies showed that there were significant differences between the Br:Bl ratios in the two species. Good CNS penetration was observed in the guinea pig and accompanied the efficacy observed in this species (Table 4), whereas poor CNS penetration in the rat was correlated

with no efficacy in the rat model. One possible explanation highlighted for this mismatch was a species difference in active transporters, although *in vitro* screening (MDR1-MDCK assay) indicated that Pgp was unlikely to be the cause. Equilibrium dialysis provided a consistent explanation for this difference between the two species.

Although the unbound fractions in brain tissue are comparable across the two species, the unbound fractions in blood are significantly different (Table 4). Poor CNS distribution in the rat could be as a result of a markedly higher degree of drug binding to blood constituents leading to a lower free fraction. It must be noted, however, that this restriction in CNS penetration is not solely the result of high affinity protein binding in blood; rather it is the result of the fact that the non-specific binding in blood greatly exceeds that in brain tissue. This difference between guinea pig blood and rat blood leads to a twenty to thirty-fold increase in the extent of protein binding in rat blood, thereby restricting the CNS penetration markedly in the rat.

Discussion

The results presented in Figures 3, 4 and 5 indicate that *in vivo* CNS penetration in the rat may be described adequately ($R^2 = 0.75$) by the use of two *in vitro* parameters, Kbb accounting for the ability of the compound to distribute into brain tissue and the efflux ratio accounting for the influence of the BBB. Thus in this current model 75% of the variance is accounted for by incorporation of Kbb and ER (Figure 4), but evidently other factors play a role. The term Kbb/ER is further expanded in equation 6:

$$\frac{Kbb}{ER} = \frac{fu(blood)}{fu(brain)} \bullet \frac{Papp(A-B)}{Papp(B-A)} \qquad (6)$$

The MDCK cell system is polarised such that Pgp acts to preferentially displace drug into the apical basin of the assay. Thus, Papp(A-B) represents transport of drug from the blood side of the BBB to the brain, while Papp(B-A) represents the converse transport from the brain back to the blood. Since the efflux experiment is performed by incubation of the drug in buffer containing no protein, the Papp values are analogous to the permeability results where fu = 1 (i.e. 100% unbound). Thus the term Kbb/ER may be interpreted as a correction of the A-B and B-A transport by their respective free concentrations in blood and brain on either side of the MDCK monolayer. Related findings in the rat were reported recently by Ohe et al. (2003) when comparing CSF-plasma ratio, plasma free fraction and Pgp efflux ratio. A strong linear correlation was observed highlighting that CSF appears to be a useful surrogate for the free brain concentration. In addition, the work of Ohe et al. (2003) suggests that the CSF concentration could be estimated from knowledge of the efflux ratio and fu(plasma). Similarly, the *in vivo* results presented in Figure 5 suggest that once the relationship between wild type, knockout mouse and efflux ratio has been established, the extent to which Pgp modulates *in vivo* CNS penetration could be estimated without the need for the knockout mouse leg of the experiment.

Optimal CNS penetration appears to be the product of the correct balance of permeability, a low propensity for active efflux and the appropriate physicochemical properties to allow partitioning into brain tissue. On the basis of the present data it appears that these factors are inter-related such that poorly permeable compounds that are also Pgp substrates may still enter the CNS if brain tissue binding provides a sufficient enough driving force to overcome the effects of the efflux transporter. Supporting this hypothesis is a recent report by Liu et al. (2005), which modelled the time required for a drug to reach equilibrium brain concentrations. The analysis showed that uptake into the brain is a hybrid function of both

permeability and fu(brain), such that poorly permeable molecules may still exhibit CNS, albeit requiring significantly longer for the compound to approach steady-state concentrations.

In terms of compound selection commonly operating in Drug Discovery, these results raise several questions about how one might apply the current permeability assays in routine screening. In a paradigm where MDR-MDCK data are generated to assess Pgp liability, would a compound be progressed into further studies if the efflux ratio were observed to be in excess of 70 and with correspondingly low passive permeability? Equally, if *in vivo* screening is employed as primary filter, would a compound showing a brain:blood ratio of 4:1 be checked for Pgp liability prior to passing onto efficacy models? Traditionally the answer to both questions would be no. Consequently, employing *in vitro* Pgp results as a hard filter may preclude the progression of potentially CNS penetrant, efficacious compounds, which may account for the fact there are so few examples currently noted of CNS penetrant Pgp substrates. Current focus should be on the use of efficacy models to aid compound selection as early as feasibly possible, in concert with free drug exposure measurements in blood and brain.

Further questions are raised by Figures 6, which highlights the trend between cLogP and log(fu(brain). As lipophilicity rises there is a general decline in the fraction of unbound drug in brain tissue, with a potential consequence that although CNS penetration may be improved by increasing lipophilicity, much of the compound will be non-specifically bound to brain tissue. Thus, the assumption that increasing lipophilicity will lead to increased efficacy for CNS compounds cannot be guaranteed and will be a balance between adequate penetration and adequate free drug in brain. A similar trend is observed between cLogP and

log(fu(blood) (data not shown). In situ brain perfusion studies have demonstrated that BBB permeability tends to increase with lipophilicity (Smith 2003), and this observation may be related to the increased propensity for binding to brain tissue, which provides the driving force for drug uptake.

Taken as a whole, the results reported here support the hypothesis that BBB transporters, permeability and free fraction in blood and brain all play a role in determining the degree of CNS penetration of a drug observed *in vivo*. Partitioning into brain tissue may act as a driving force to overcome at least some of the effects of efflux transporters at the blood-brain barrier, by supplying a sufficiently large concentration gradient to promote CNS penetration. Thus it cannot be assumed that because a compound is a substrate for Pgp it cannot gain access to the brain. Equally, the use of equilibrium dialysis allows for a high capacity means of assessing free drug fractions in blood and brain tissue, and the opportunity to investigate species differences in CNS penetration. Further work is required to understand the role of other drug transporters in CNS disposition (i.e. BCRP) and also in the applicability of estimating fu(brain) to understanding drug efficacy at the level of the brain, where local free concentrations may differ from that in the bulk milieu.

Acknowledgements

The authors would like to thank David Begley for his assistance and advice during their preparation of this manuscript. In addition the following people are acknowledged for the contributions, Ann Lewis, Ian Owens, Jonathan Barford, Paul Goldsmith, Lee Abberley, Beverly Smith, Caroline Peet, Michael Briggs, Colin Howes, Lee Skinner, Teresa Heslop, Ann Metcalf, Joanne Schogger, Trevor White, Nigel Deeks, Tania Buck and Evangelia Grigorakou.

References

Artursson P (1990) Epithelial transport of drugs in cell culture. I: A model for studying the passive diffusion of drugs over intestinal absorptive (caco-2) cells. J Pharm Sci 79:476-482.

Benet LZ, Kroetz DL, Sheiner LB (1996) Pharmacokinetics The dynamics of drug absorption, distribution and elimination in Goodman and Gilman's the pharmacological basis of therapeutic (Hardman GH, Limbird LE eds) pp 3-28, McGraw-Hill, New York.

Brown EA, Griffiths R, Harvey CA, Owen DA (1986) Pharmacological studies with SK&F93944 (Temelastine) a novel histamine H1-receptor antagonist with negligible ability to penetrate the central nervous system. Br J Pharmacol 87:569-578.

Clark DE (1999) Rapid calculation of polar molecular surface area and its application to the prediction of transport phenomena. 2. Prediction of blood-brain barrier penetration. J Pharm Sci 88: 815-821.

De Lange ECM, Danhof M, de Boer AG, Breimer DD (1997) Methodological considerations of intercerebral microdialysis in pharmacokinetic studies on drug transport across the blood brain barrier. Brain Res Rev 25:27-49.

Doran A, Obach RS, Smith BJ, Hosea NA, Becker S, Callegari E, Chen C, Chen X, Choo E, Cianfrogna J, Cox LM, Gibbs JP, Gibbs MA, Hatch H, Hop CECA, Kasman IN, LaPerle J, Lui J, Liu X, Logman M, Maclin D, Nedza FM, Nelson F, Olson E, Rahematpura S, Raunig D, Rogers S, Schmidt K, Spracklin DK, Szewc M, Trouman M, Tseng E, Tu M, van Deusen JW, Venkatakrishnan K, Walens G, Wang, EQ, Wong D, Yasgar AS, Zhang C (2005) The

impact of P-glycoprotein on the disposition of drugs targeted for indications of the central nervous system: evaluation using the mdr1a/b knockout mouse model. Drug Metab Dispos 33:165-174.

Kalvass JC, Maurer TS (2002) Influence of non-specific brain and plasma binding on CNS exposure: implications for rational drug discovery. Biopharm Drug Dispos 23:327-338.

Kuresh AY, Qaiser MZ, Begley DJ, Rice-Evans CA, Abbot NJ (2004) Flavonoid Permeability Across an In Situ Model of the Blood-Barrier. Free Radic Biol Med 36:592-604.

Langer O, Muller M (2004) Methods to assess tissue-specific distribution and metabolism of drugs. Curr Drug Metab 5:463- 481.

Lentz KA. Polli JW. Wring SA. Humphreys JE. Polli JE (2000) Influence of passive permeability on apparent P-glycoprotein kinetics, Pharm Res (NY) 17:1456-1460.

Lin JH (2004) How significant is the role of P-glycoprotein in drug absorption and brain uptake. Drugs of Today 40:5-22.

Lin JH, Yamazaki M (2003) Clinical relevance of P-glycoprotein in drug therapy. Drug Metab Rev 35:417-454.

Liu X, Smith BJ, Chen C, Callegari E, Becker SL, Chen X, Cianfrogna J, Doran AC, Doran SD, Gibbs JP, Hosea N, Liu J, Nelson FR, Szewc MA, Van Deusen J (2005) Use of a Physiologically Based Pharmacokinetic Model to Study the Time to Reach Brain

Equilibrium: An Experimental Analysis of the Role of Blood-Brain Barrier Permeability, Plasma Protein Binding, and Brain Tissue Binding. J Pharmacol Exp Ther 313: 1254-1262.

Mahar Doan KM, Humphreys JE, Webster LO, Wring SA, Shampine LJ, Serabjit-Singh CJ, Adkikison KK, Polli JW (2002) Passive Permeability and P-Glycoprotein-Mediated Efflux Differentiate Central Nervous System (CNS) and Non-CNS Drugs. J Pharmacol Exp Ther 303:1029-1037.

Maurer TS, DeBartolo DB, Tess DA, Scott DO (2005) Relationship between exposure and nonspecific binding of thirty-three central nervous system drugs in mice. Drug Metab Dispos 33:175-181.

Ohe T, Sato M, Tanaka S, Fujino N, Hata M, Shibata Y, Kanatani A, Fukami M, Yamakazi M, Chiba M, Ishii Y (2003) Effect of P- glycoprotein mediated efflux on cerebrospinal fluid/plasma concentration ratio. Drug Metab Dispos 31:1251-1254.

Pascual J, Munoz P (2005) Correlations between lipophilicty and triptan outcomes. Headache 45:3-6.

Shen DD, Artru AA, Adkinson KK (2004) Principles and applicability of CSF sampling for the assessment of CNS drug delivery and pharmacodynamics. Adv Drug Delivery Rev 56:1825-1857.

Smith QR (2003) A review of blood-brain barrier transport techniques, in The blood-brain barrier (Nag S, eds), pp 193-207, Humana Press, Totawa, New Jersey

Wang Q, Rager JD, Weinstein K, Kardos PS, Dobson GL, Li J, Hidalgo IJ (2005) Evaluation of the MDR-MDCK cell line as a permeability screen for the blood-brain barrier. Int J Pharm 288:349-359.

Legend for Figures

Fig. 1a. Plot of *in vivo* Br:Bl ratio in rat versus free fraction in rat blood. Pgp substrates are highlighted separately (○). Least squares linear regression yields the relationship, y = 1.5636x + 0.7339, R^2 = 0.0492 (all compound data points included).

Fig. 1b. Plot of *in vivo* Br:Bl ratio versus Kbb in rat. Pgp substrates are highlighted separately (○). Least squares linear regression yields the relationship, y = 0.8115x - 0.0081, R^2 = 0.5448 (non PgP substrates only), y = 0.3877x + 0.3129, R^2 = 0.1954 (all compound data points included).

Fig. 2. Log(fu) in brain plotted against log fu in blood. Acidic compounds (calculated pKa less than pH 7.4) are highlighted (▲), Pgp substrates are highlighted (○). For the non-acid series, least squares linear regression substrates yields the relationship, y = 1.0685x + 0.0403, R^2 = 0.8161. For the acidic series, least squares linear regression substrates yields the relationship, y = 0.0666x + 0.0011, R^2 = 0.6664 (GSK-15 is a zwitterion and was excluded from regression analysis).

Fig. 3. Graph showing the incorporation of two *in vitro* parameters (Kbb and efflux ratio) to correlate with *in vivo* Br:Bl ratio.

Fig. 4. Graph showing plot of Kbb versus *in vivo* Br:Bl ratio, with Pgp substrates corrected for efflux ratio. Least squares linear regression yields the relationship, y = 0.9415x - 0.1282, R^2 = 0.7465 (all compound data points)

Fig. 5. Graph showing a plot of Br:Bl ratios in mdr1a/b(+/+) mice versus brain:blood ratios in mdr1a/b(-/-) mice corrected by efflux ratio (ER) to account for the role of Pgp in modulating CNS penetration.

Fig. 6. Log(fu) in brain plotted versus cLogP for compounds presented in Table 2. Acidic compounds (calculated pKa less than pH 7.4) are highlighted (▲), Pgp substrates are highlighted (○). Least squares linear regression yields the relationship, $y = -0.0499x + 0.3058$, $R^2 = 0.3733$ (all compound data points).

JPET Fast Forward. Published on December 5, 2005 as DOI: 10.1124/jpet.105.092916
This article has not been copyedited and formatted. The final version may differ from this version.

TABLE 1

Summary of unbound drug fractions (n = 6) in blood and brain homogenate, *in vitro* Br:Bl partition ratio (Kbb), *in vivo* Br:Bl ratio (n = 3), calculated logP (cLogP) and calculated pKa (ApKa).

Name	fu (blood)		fu (brain)		Kbb		Br:Bl ratio[b]		cLogP	ApKa
	Mean	S.D.	Mean	S.D.	Mean	Range[a]	Mean	S.D.		
GSK-1	0.2130	0.0169	0.0701	0.0022	3.04	2.59 - 3.47	4.00	0.44	3.51	-
GSK-2	0.1738	0.0186	0.0581	0.0027	2.99	2.36 - 3.69	0.50	0.10	2.75	-
GSK-3	0.1754	0.0112	0.0460	0.0010	3.82	3.32 - 4.26	0.50	0.10	3.66	-
GSK-4	0.0135	0.0035	0.0090	0.0024	1.49	0.82 - 2.73	0.05	0.02	4.59	7.84
GSK-5	0.0399	0.0030	0.0069	0.0002	5.75	4.98 - 6.70	0.14	0.03	5.45	11.92
GSK-6	0.0751	0.0068	0.0137	0.0012	5.47	4.36 - 6.73	0.28	0.01	1.16	-
GSK-7	0.5517	0.0481	0.4674	0.0308	1.18	0.98 - 1.41	0.07	0.01	0.31	-
GSK-8	0.0234	0.0015	0.0178	0.0109	1.31	1.13 - 1.45	0.03	0.01	3.99	-
GSK-9	0.3303	0.0227	0.1831	0.0135	1.80	1.46 - 2.11	1.53	0.21	2.02	-
GSK-10	0.3119	0.0334	0.1711	0.0108	1.82	1.46 - 2.31	2.54	0.33	2.33	-
GSK-11	0.00479	0.00025	0.0188	0.0020	0.25	0.21 - 0.34	0.01	<0.01	4.91	4.3
GSK-12	0.00168	0.00056	0.0261	0.0038	0.06	0.04 - 0.13	0.02	<0.01	4.15	4.2
GSK-13	0.00078	0.00006	0.00236	0.00015	0.33	0.28 - 0.41	0.20	0.03	7.14	0.96
GSK-14	0.00021	0.00006	0.00047	0.00006	0.46	0.23 - 0.75	0.01	<0.01	6.80	1.25
GSK-15	0.4333	0.1062	0.2587	0.0534	1.67	1.01 - 3.17	0.50	0.73	-1.90	1.53
GSK-16	0.00029	0.00003	0.00371	0.00020	0.08	0.06 - 0.09	0.02	0.01	7.30	2.73
GSK-17	0.00207	0.00014	0.00225	0.00025	0.92	0.72 - 1.15	0.53	0.04	6.34	3.09
GSK-18	0.00009	0.00000	0.00006	0.00001	1.38	0.53 - 1.03	0.93	n/a	7.88	3.09
GSK-19	0.00047	0.00009	0.00089	0.00015	0.53	0.33 - 0.82	0.18	n/a	7.14	3.09
GSK-20	0.00031	0.00009	0.00027	0.00007	1.14	0.56 - 2.35	0.52	n/a	7.27	3.18
GSK-21	0.00139	0.00009	0.00152	0.00020	0.92	0.73 - 1.22	0.35	0.04	6.52	3.22
GSK-22	0.00062	0.00004	0.00165	0.00008	0.38	0.33 - 0.43	0.18	0.02	7.63	3.66
GSK-23	0.00309	0.00033	0.06684	0.00893	0.05	0.04 - 0.07	0.02	0.01	4.66	4.53
GSK-24	0.0576	0.0024	0.0340	0.0012	1.70	1.55 - 1.91	1.05	0.32	3.57	-
GSK-25	0.00950	0.00114	0.00601	0.00100	1.58	0.95 - 2.31	0.80	0.20	3.53	-
GSK-26	0.00216	0.00029	0.00066	0.00011	3.27	2.06 - 4.17	3.25	0.55	4.82	-
GSK-27	0.0151	0.0013	0.0050	0.0012	3.01	2.53 - 4.33	3.16	0.04	3.71	-
GSK-28	0.00892	0.00131	0.00312	0.00082	2.86	2.35 - 3.71	3.42	0.02	3.50	-
GSK-29	0.0338	0.0040	0.0289	0.0048	1.17	1.00 - 1.45	1.43	0.11	1.99	-
GSK-30	0.0407	0.0041	0.0374	0.0079	1.09	0.96 - 1.28	0.67	0.19	3.10	-
GSK-31	0.0348	0.0027	0.0115	0.0018	3.02	2.55 - 3.30	1.53	0.40	3.86	-

JPET Fast Forward. Published on December 5, 2005 as DOI: 10.1124/jpet.105.092916
This article has not been copyedited and formatted. The final version may differ from this version.

GSK-32	0.00044	0.00005	0.00044	0.00007	0.99	0.66 - 1.35	0.47	n/a	6.76	-
GSK-33	0.00072	0.00009	0.00030	0.00008	2.38	1.28 - 3.23	3.40	n/a	5.87	-
GSK-34	0.00158	0.00013	0.00095	0.00011	1.66	1.28 - 2.06	2.20	0.27	5.47	-
GSK-35	0.0023	0.0005	0.0006	0.0001	3.74	2.54 - 5.83	0.37	n/a	5.05	-
GSK-36	0.4398	0.0624	0.3551	0.0866	1.24	0.71 - 1.93	4.04	0.49	2.73	-
GSK-37	0.00060	0.00013	0.0151	0.0091	0.04	0.03 - 0.05	0.05	0.02	4.97	-
GSK-38	0.00041	0.00022	0.0113	0.0050	0.04	0.03 - 0.04	0.05	0.02	3.75	-
GSK-39	0.00107	0.00129	0.0126	0.0073	0.08	0.07 - 0.11	0.05	<0.01	4.49	-
GSK-40	0.4762	0.0241	0.2824	0.0630	1.69	1.26 - 2.62	1.20	0.20	3.17	-
GSK-41	0.3968	0.0343	0.2780	0.0464	1.43	0.91 - 2.04	1.83	0.20	5.30	-
Naproxen	0.0180	0.0013	0.5416	0.1173	0.03	0.03 - 0.04	0.02	0.01	2.82	4.06
Ibuprofen	0.0160	0.0026	0.2964	0.0809	0.05	0.05 - 0.07	0.03	0.02	3.68	4.08
Indomethacin	0.00571	0.00074	0.0592	0.0055	0.10	0.08 - 0.12	0.01	<0.01	4.18	4.26
Diclofenac	0.0118	0.0018	0.0547	0.0101	0.22	0.16 - 0.31	0.02	0.01	4.73	4.48
Ketorolac	0.0582	0.0046	0.4853	0.1144	0.12	0.09 - 0.15	0.01	<0.01	1.62	3.63
Flurbiprofen	0.00627	0.00027	0.1289	0.0189	0.05	0.04 - 0.05	0.01	<0.01	3.75	3.03
Ciglitazone	0.00103	0.00010	0.00034	0.00010	3.00	1.72 - 4.42	2.10	0.24	5.07	7.17
Pioglitazone	0.00657	0.00022	0.02304	0.00219	0.28	0.25 - 0.34	0.16	0.02	3.53	7.24
Celecoxib	0.00116	0.00013	0.00345	0.00086	0.34	0.28 - 0.40	0.14	<0.01	4.37	8.83
Valdecoxib	0.00762	0.00353	0.0339	0.0041	0.23	0.20 - 0.26	0.05	0.01	1.83	9.49
Paracetamol	0.6849	0.0951	0.8327	0.1521	0.82	0.54 - 1.39	0.07	0.05	0.49	10.12
Vioxx	0.2944	0.0233	0.2746	0.0215	1.07	0.88 - 1.41	0.80	0.03	1.80	-
Aricept	0.2853	0.0561	0.1023	0.0103	2.79	1.90 - 3.97	3.45	0.16	4.60	-
Etoricoxib	0.2558	0.0161	0.1502	0.0283	1.70	1.45 - 2.09	0.66	0.04	2.35	-
risperidone	0.1089	0.0142	0.1438	0.0185	0.76	0.53 - 1.05	0.30	0.04	2.71	-

[a] Variability in Kbb values was assessed as follows: lower limit calculated using the lowest fu(blood) replicate divided by the highest fu(brain) replicate, upper limit calculated using the highest fu(blood) replicate divided by fu(brain) replicate.

[b] Br:Bl ratios were derived for acute studies for GSK-2, GSK-16, GSK-24, GSK-25, GSK-32, GSK-33, GSK-34, GSK-35 and GSK-36. Br:Bl ratios for the following compounds were derived from n = 1 studies, GSK-18, GSK-19, GSK-20, GSK-32, GSK-33 and GSK-35

TABLE 2

Summary of permeability (n = 3), efflux data and unbound drug fractions in blood and brain homogenate (n = 6)

Name	Papp (nm/s), without GF120918					Mean (nm/s), with GF120918					*In vitro corrections*	
	A-B (nm/sec)		B-A (nm/sec)		Efflux ratio (ER)	A-B (nm/sec)		B-A (nm/sec)		Efflux ratio (ER)	Kbb / ER	Kbb[a]
	Mean	S.D.	Mean	S.D.		Mean	S.D.	Mean	S.D.			
GSK-1	58.1	12.1	502.3	28.6	8.7	168.3	38.1	227.0	20.5	1.3	0.351	3.56
GSK-2	7.2	1.2	539.3	51.0	74.9	158.0	7.5	105.3	4.7	0.7	0.040	0.23
GSK-3	9.0	1.8	606.3	60.1	67.6	68.7	2.4	56.7	14.8	0.8	0.056	0.41
GSK-4	2.3	0.6	288.7	26.3	125.5	14.7	2.1	18.3	2.5	1.2	0.012	-0.07
GSK-5	5.0	1.0	599.7	65.5	120.7	41.9	8.1	49.4	2.6	1.2	0.048	0.31
GSK-6	11.3	1	778.4	90.6	68.9	249.9	7.2	188.9	14.0	0.8	0.079	0.66
GSK-7	8.3	0.6	486.3	57.8	58.8	71.8	2.0	100.2	5.3	1.4	0.020	0.02
GSK-8	9.8	1.3	730.6	26.6	74.3	154.9	6.5	184.5	8.9	1.2	0.018	-0.01
GSK-9	47.9	4.4	633.7	39.8	13.2	220.0	21.6	192.6	43.9	0.9	0.136	1.27
GSK-10	113.8	33	763.4	33.3	6.7	349.1	29.1	383.5	18.1	1.1	0.272	2.71
GSK-11	103	8.1	1102.2	117.2	10.7	317.5	17.8	200.1	37.5	0.6	0.024	0.06
GSK-40	4.27	0.39	35.6	7.8	8.3	21.8	1.4	15.7	1.8	0.7	0.202	1.97
GSK-41	66.1	3.9	547.0	24.0	8.3	229.0	4.2	252.7	24.0	1.1	0.172	1.65
Risperidone	36.0	1.0	748.4	64.0	20.8	300.3	27.9	308.6	12.1	1.0	0.036	0.20

a Pgp substrate correction for Kbb using the regression line derived from Figure 4 (i.e. $Y = 10.707X - 0.1949$ ($R^2 = 0.9342$), where Y is taken as the Pgp corrected Kbb and X represents the term Kbb/ER.

JPET Fast Forward. Published on December 5, 2005 as DOI: 10.1124/jpet.105.092916
This article has not been copyedited and formatted. The final version may differ from this version.

TABLE 3

Summary of *in vivo* Br:Bl ratios (n = 3) measured in mdr1a/b(+/+) and mdr1a/b(-/-) mice together with correction for efflux ratio.

Name	Br:Bl ratio mdr1a/b (+/+)		Br:Bl ratio mdr1a/b(-/-)		Efflux ratio	Br:Bl ratio mdr1a/b(-/-)/ER
	Mean	SD	Mean	SD		
GSK-1	4.07	0.14	10.72	0.75	8.7	1.2322
GSK-2	0.53	0.05	15.50	1.35	68	0.2293
GSK-3	1.10	0.06	14.34	2.07	68	0.2118
GSK-4	0.07	0.01	1.43	0.10	126	0.0114
GSK-5	0.11	0.01	3.88	0.19	121	0.0321
GSK-9	0.93	0.04	5.47	0.19	13	0.4144
GSK-10	2.29	0.25	4.18	0.12	7	0.6239
GSK-40	0.80	0.00	3.40	0.20	8.3	0.4096
GSK-41	1.28	0.07	4.49	0.21	8.3	0.5410
GSK-42	5.45	0.06	12.95	0.19	8.2	1.5793
GSK-43	0.56	0.08	15.36	1.17	56	0.2753
GSK-44	0.012	0.01	0.21	0.01	52	0.0040
GSK-45	0.04	<0.01	0.75	0.03	52	0.0145
GSK-46	1.84	0.38	12.36	1.68	32	0.3827
GSK-47	0.04	0.01	0.24	0.17	24	0.0102
GSK-48	0.1	0.01	0.81	0.21	31	0.0261
GSK-49	0.047	0.014	0.22	0.03	4.9	0.0449
GSK-50	0.08	0.01	0.35	0.04	10.9	0.0321
Risperidone	0.44	0.17	5.52	0.75	21	0.2654
Loperamide	0.08	0.03	2.61	0.7	43	0.0607
Digoxin	0.05	0.01	1.4	0.1	28	0.0500

TABLE 4

Comparison of unbound drug fractions (n = 6) and *in vivo* Br:Bl ratios (n = 3) for three compounds in the rat and guinea pig.

Name	Species	fu (blood)		fu(brain)		Kbb		Br:Bl ratio	
		Mean	S.D	Mean	S.D.	Mean	Range	Mean	S.D.
GSK-37	Rat	0.00060	0.00013	0.0151	0.0091	0.04	0.03 – 0.05	<0.05	<0.01
GSK-38	Rat	0.00041	0.00022	0.0113	0.0050	0.04	0.03 – 0.04	<0.05	<0.01
GSK-39	Rat	0.00107	0.00129	0.0126	0.0073	0.08	0.07 – 0.11	<0.05	<0.01
GSK-37	Guinea Pig	0.0218	0.0226	0.0181	0.0154	1.2	0.94 – 1.55	1.60	0.08
GSK-38	Guinea Pig	0.0184	0.0011	0.0140	0.0024	1.3	0.97 – 1.86	1.26	0.19
GSK-39	Guinea Pig	0.0251	0.0011	0.0128	0.0007	2.0	1.76 – 2.30	1.21	0.05

JPET Fast Forward. Published on December 5, 2005 as DOI: 10.1124/jpet.105.092916
This article has not been copyedited and formatted. The final version may differ from this version.

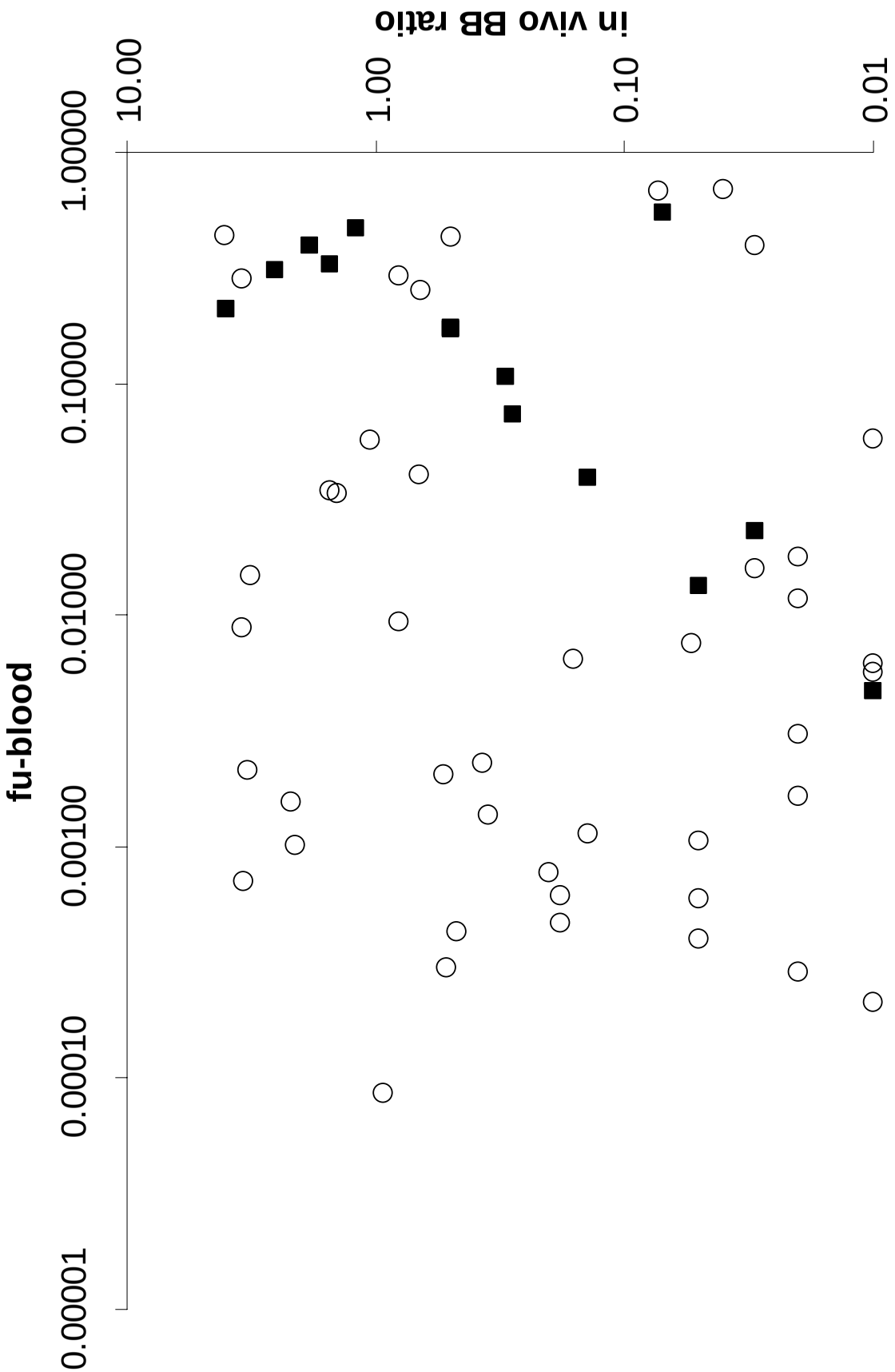

Figure 1a

JPET Fast Forward. Published on December 5, 2005 as DOI: 10.1124/jpet.105.092916
This article has not been copyedited and formatted. The final version may differ from this version.

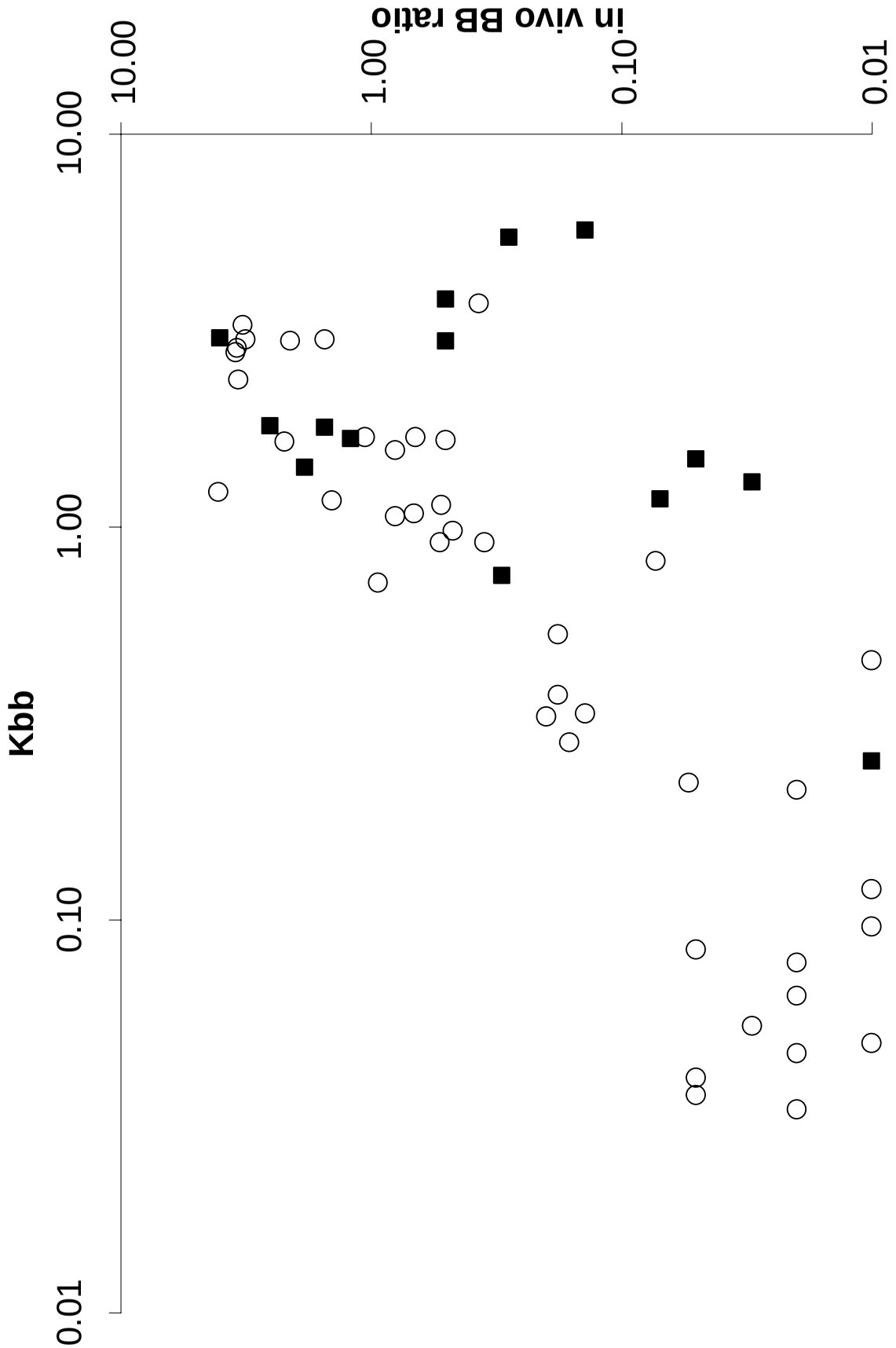

Figure 1b

JPET Fast Forward. Published on December 5, 2005 as DOI: 10.1124/jpet.105.092916
This article has not been copyedited and formatted. The final version may differ from this version.

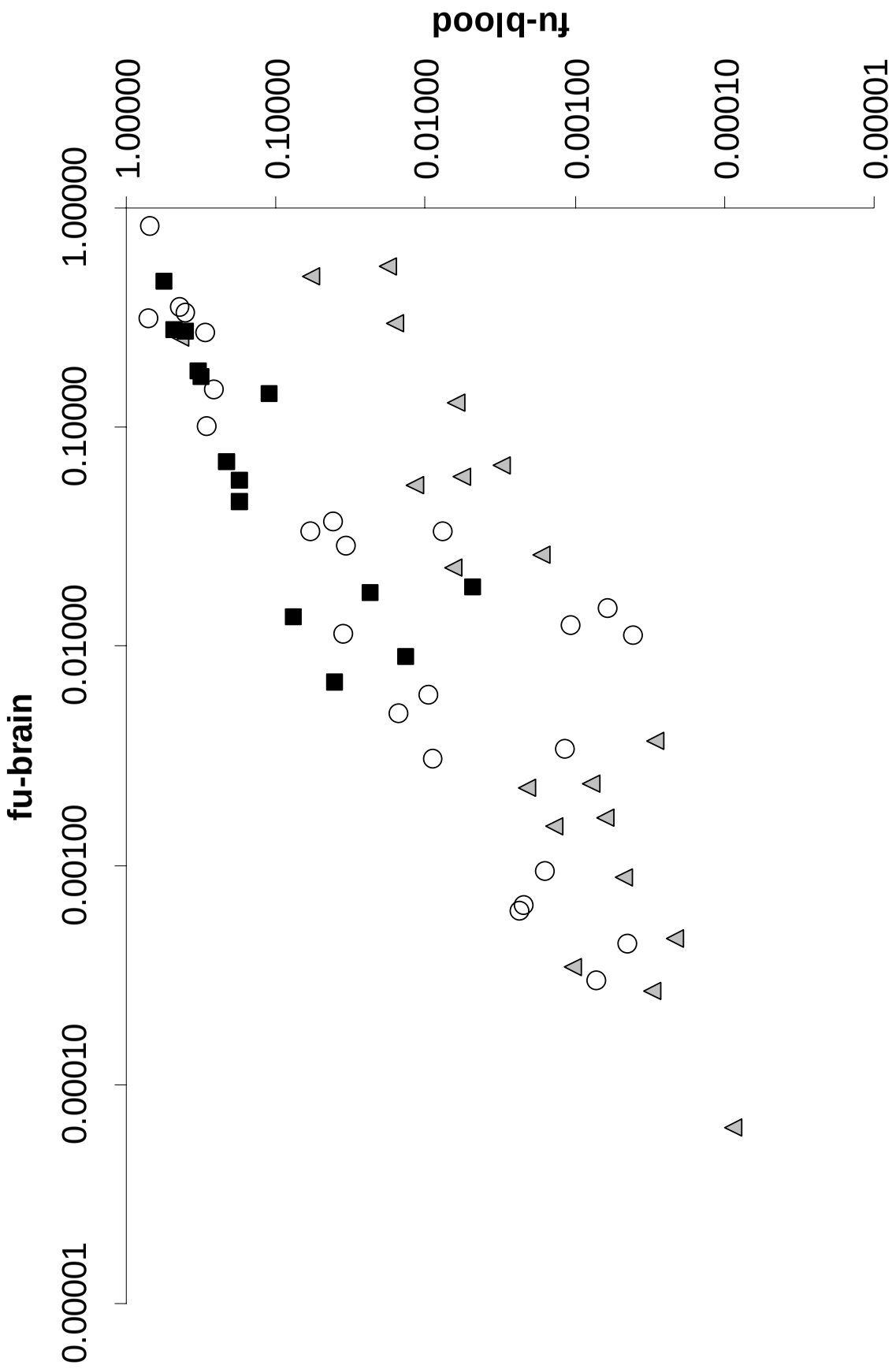

Figure 2

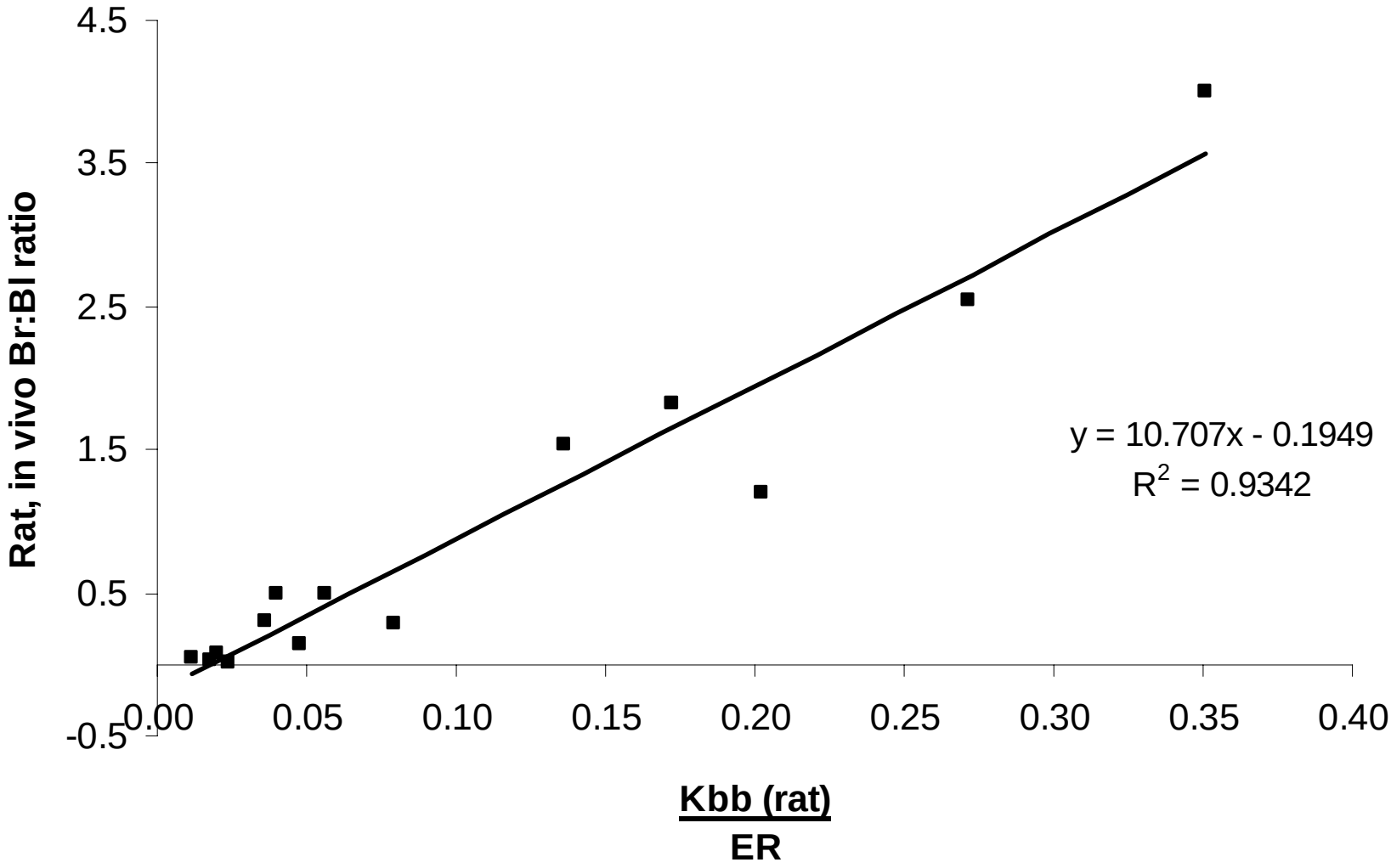

Figure 3

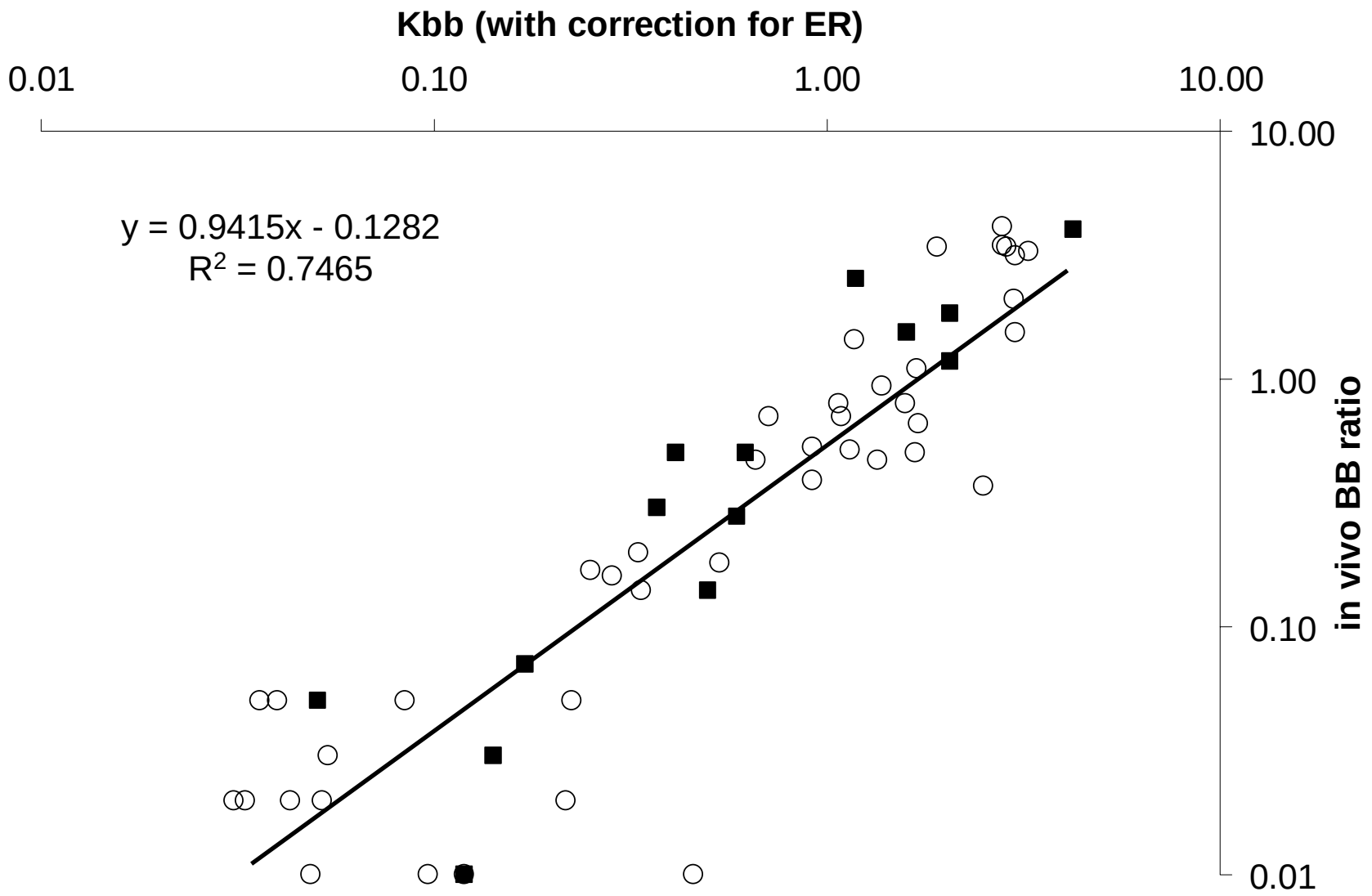

Figure 4

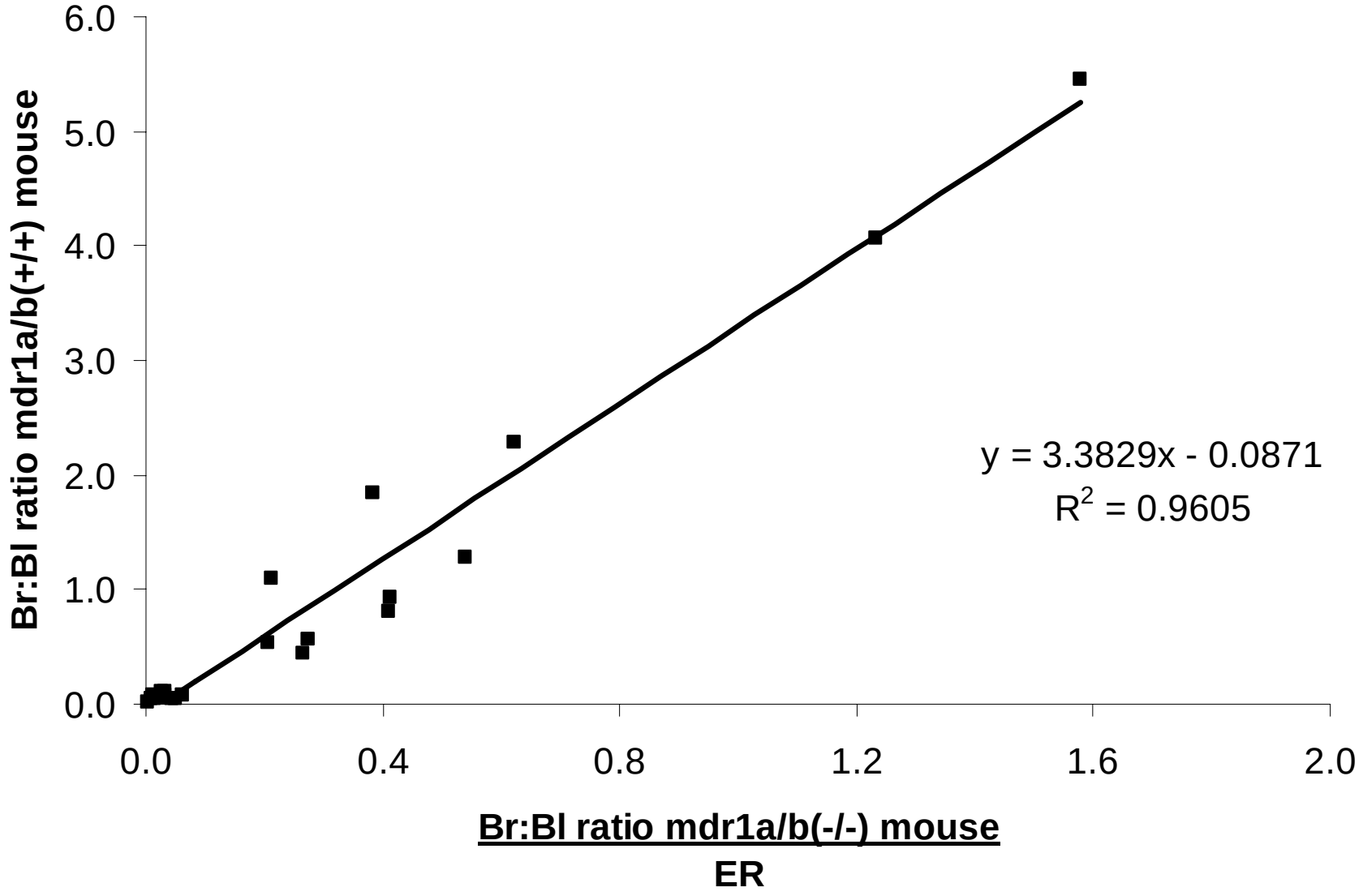

Figure 5

JPET Fast Forward. Published on December 5, 2005 as DOI: 10.1124/jpet.105.092916
This article has not been copyedited and formatted. The final version may differ from this version.

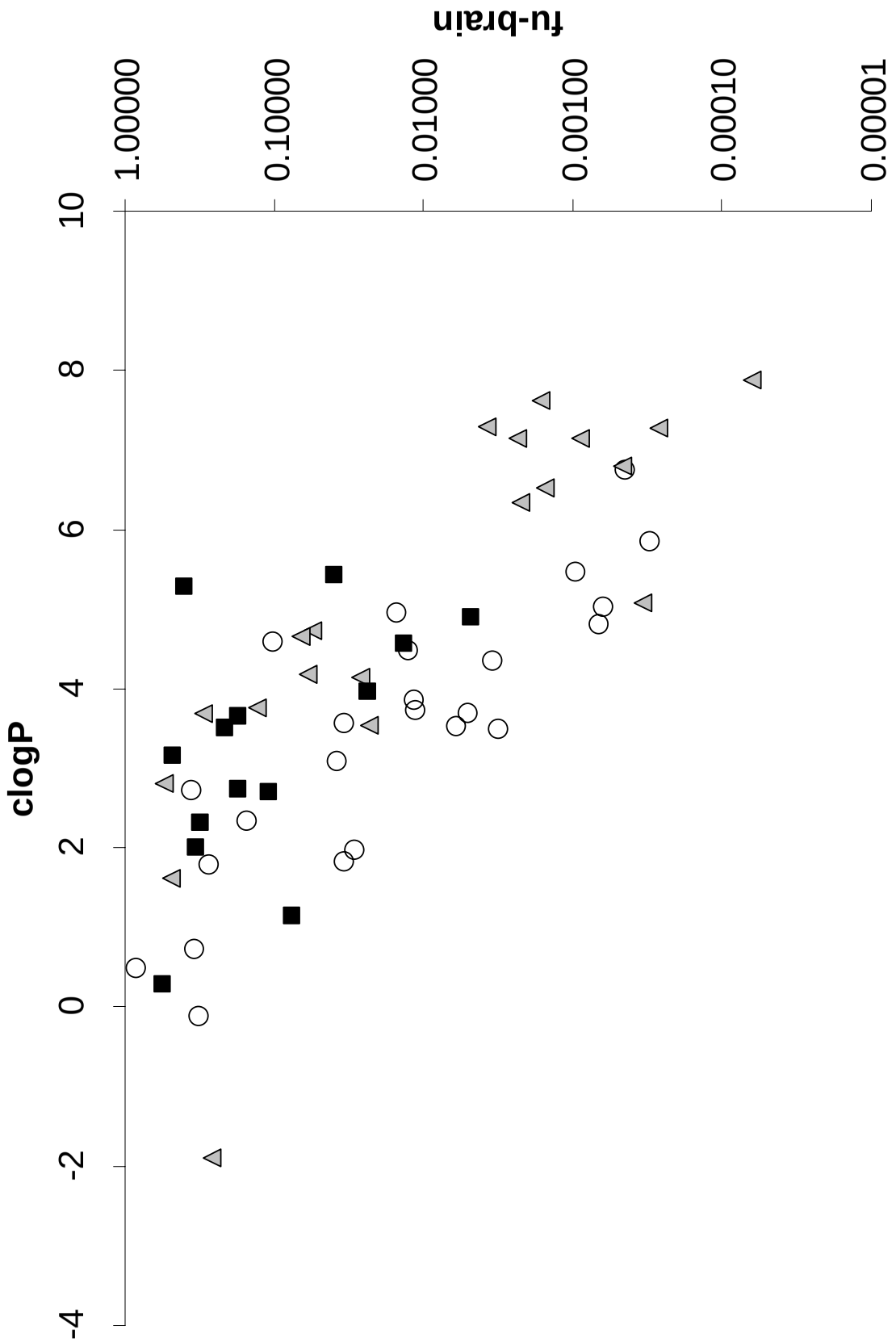

Figure 6